PHYSICAL REVIEW E **82**, 010302(R) (2010)

Granular dynamics of a slurry in a rotating drum

C. C. Liao,[1] S. S. Hsiau,[1] and Kiwing To[2]
[1]*Department of Mechanical Engineering, National Central University, Jhongli, Taiwan 32001, Republic of China*
[2]*Institute of Physics, Academia Sinica, Taipei, Taiwan 115, Republic of China*
(Received 23 March 2010; published 30 July 2010)

We study the effects of interstitial fluid viscosity on the rates of dynamical processes in a thin rotating drum half-filled with monodisperse glass beads. The rotating speed is fixed at the rolling regime such that a continuously flowing layer of beads persists at the free surface. While the characteristic speed of a bead in the flowing layer decreases with the fluid viscosity μ, the mixing rate of the beads is found to increase with μ. These findings are consistent to a simple model related to the thickness of the flowing layer. In addition, our results indicate a possible transition from the inertial limit regime to the viscous limit regime (reported previously by S. Courrech du Pont *et al.* [Phys. Rev. Lett. **90**, 044301 (2003)]) when the Stokes number is reduced.

DOI: 10.1103/PhysRevE.82.010302 PACS number(s): 45.70.Mg, 47.51.+a, 45.70.Vn

It is generally accepted that the dynamical processes in a fluid system are slowed down by the viscous drag of the fluid. For example, the diffusion rate of a Brownian particle in a fluid decreases with increasing fluid viscosity. Hence, in a system consists of two kinds of particles initially segregated, the mixing rate of these particles via diffusion should be slower in a more viscous fluid. However, we find that mixing of granular materials in a rotating drum behaves differently.

Rotating drum has become a popular experimental device to investigate the physics of granular flow because of its simple closed geometry, and its practical use in many industrial processes for drying, segregation and mixing of granular materials [1–4]. Depending on the rotation speed, material filling fraction, and drum diameter, different flow regimes such as: avalanching, rolling, cascading, cataracting, and centrifuging may occur in dry granular materials [4]. In the rolling regime at a low enough speed, one always observes two distinct regions in the drum [see Fig. 1(a)]: a fixed bed region in which the material undergoes solid rotation with the drum, and a thin layer region at the free surface in which mixing and segregation of the granular material take place. It had been reported that mixing of large and small glass beads was better when the drum was filled with water instead of air [5]. However, the mixing mechanism was not well understood, possibly due to the presence of size segregation and mixing simultaneously in their system. So, in order to investigate the effect of interstitial fluid on the mixing dynamics, it will be better to consider granular systems of identical particles with no drive for segregation.

In the presence of a fluid, a moving grain experiences a buoyant force as well as a fluid drag force. While the effect of buoyancy may be taken care of by rescaling gravity, the fluid drag force may change the nature of the grain dynamics qualitatively. For a rotating drum running in discrete avalanches flow, Courrech du Pont *et al.* [6] studied the statistics of the avalanche duration and found a transition from a viscous regime to an inertial regime and then to a free-fall regime when the Stokes number increased. Since the fluid drag force acts on individual grains, it may be possible to observe these transitions even when the drum is running in a continuous flow.

In this study, we have performed experiments to investigate the effect of the interstitial fluid viscosity μ on the granular dynamics of a slurry of monodisperse particles in a rotating drum operating in the rolling regime. We find that the characteristic flow speed decreases with μ, whereas the particle mixing rate increases with μ. Such a finding is consistent with a simple model in terms of the size of the mixing region. In addition, when the Stokes number increases the characteristic flow speed data suggests a viscous to inertia transition [6] which is further supported by the measurements of the mixing rate.

The experimental setup is shown schematically in Fig. 1(a). A transparent water proof quasi-two-dimensional (quasi-2D) drum of $R=10$ cm radius and $w=2.5$ cm axial gap width is constructed using Plexiglass. We half-fill the drum with glass beads of density $\rho=2.5$ g/cm^3 and diameter $d=3\pm0.1$ mm. The bead diameter is less than one eighth of the gap width so that the effect of the side wall on the bead dynamics may be ignored [6,7]. Half of the glass beads are black and the other half are white with all the white beads loaded at the bottom as the initial configuration. Then the drum is completely filled with water-glycerin mixture before it is sealed. By using air and water-glycerin mixture of different glycerin weight fraction f, we vary μ from 0.02 mPa s (air) to 1.41Pa s (pure glycerin, $f=1$). Our laboratory is kept at 20 ± 0.5 °C when the experiments are performed. We set the rotation speed Γ to 2.3rpm so that a continuous flow is maintained at the free surface. A digital camera (Sony DCR-TRV900 NTSC) is used to capture high resolution images (400×400 pixel^2 spatial resolution) at 30 fps. In addition, we use another camera (IDT X-3 plus) to record high-speed images (1000 fps at 240×240 pixel^2) for measuring the steady state flow field in a region [the dotted square in Fig. 1(a)] near the center of the drum.

Figures 1(b)–1(d) show the high-resolution images taken at different times in an experiment for the dry system. While the free-surface inclination angle θ reaches its steady state value in less than one revolution, complete mixing of the beads takes about 12 revolutions. However, the free-surface of the slurry with the high glycerin concentration ($f=0.85$) is curved into an "S"-shape as shown in Fig. 1(f). In the case of pure glycerin the free surface no longer exists and the slurry

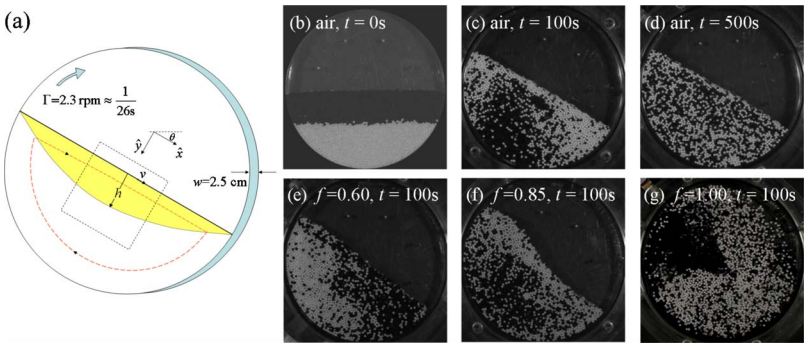

FIG. 1. (Color online) (a) A schematic diagram of the rotating drum. The shaded (yellow online) region is where beads are mixed. (b)–(g) Images captured at different time: (b) $t=0$ s; (c) $t=100$ s; (d) $t=500$ s for the dry system (upper row) and for (e) $f=0.60$, (f) $f=0.85$, (g) $f=1.00$ at $t=100$ s (lower row). The physical dimensions of images (b)–(g) are 20×20 cm^2.

becomes a suspension as shown in Fig. 1(g). Clearly, the dynamics of the high glycerin concentration slurries are different from those when $f<0.85$. In this paper, we shall focus on the experiments for $0<f\leq0.80$. Within this range of f, the fluid viscosity μ increases from 1 mPa s to 60.1 mPa s. On the other hand, the density of the fluid ρ_f increases from 1.00 g/cm^3 (pure water) to 1.20 g/cm^3 ($f=0.80$) and the density difference $\Delta\rho=(\rho-\rho_f)$, which denotes the buoyant effect, changes from 1.50 g/cm^3 to 1.30 g/cm^3. Since the dynamics of the slurry depend on the Stokes number St $\propto\sqrt{\Delta\rho}/\mu$ [6], one can compare the effect of buoyancy and fluid viscosity on the slurry dynamics in terms of the fractional change $\frac{\Delta St}{\langle St\rangle}$. The quantity $\frac{\Delta St}{\langle St\rangle}$ equals 0.072 and 1.93 due to changes in $\Delta\rho$ and μ, respectively. Hence the effect of the fluid density variations on the bead dynamics may be neglected.

From visual observation, a bead in different parts of the drum moves in different manners. In the lower region away from the free surface, all the beads circle the center of the drum with the same angular velocity. The beads pack as a whole performs solid rotation without relative motion. When a bead is close to the free surface, it flows with an average velocity that decreases with the depth from the free surface. Hence, the slurry may be partitioned into a fluidized region [shaded region in Fig. 1(a)] near the free surface and a solid rotation region. Since mixing of the beads occurs mainly in the fluidized region, we call this region the mixing region hereafter.

A quantitative measure of the size of the mixing region can be obtained by analyzing the average flow field from the high-speed images. In brief, particle tracking velocimetry technique is used to locate the centers of the white beads in the high speed images and to determine the displacements of the beads between two consecutive images. Then the velocity of the bead is calculated and the flow field is obtained by averaging the velocities in a region of 3×3 mm^2. Figure 2(a) shows a typical flow field measured in a region [dotted square in Fig. 1(a)] of 4.8×4.8 cm^2 near the center of the drum. Each arrow in the flow field is an average of at least 400 beads. Let $v(y)$ denote the mean velocity in the x direction of the beads at a distance y from the free surface. The velocity profile $v(y)$ along the line passing through the center decreases with y as shown in Fig. 2(b). The surface flow velocity v_s decreases linearly with μ for small μ and inversely for large μ as shown in Fig. 3(a). Except for the dry system, which appears to belong to a different regime, v_s can be fitted to an empirical form: $v_s=\frac{a}{1+\mu/b}$ with $a=6.1$ cm/s and $b=139$ mPa s. The thickness h, such that $v(h)$ is the last value before $v(y)$ becomes negative, is a measure of the size of the mixing region and the mean flow velocity $\langle v\rangle\equiv h^{-1}\int_h^0 v(y)dy$ is a characteristic speed of the beads in the mixing region.

Note that h and $\langle v\rangle$ are related by mass conservation. Let n be the number of the beads per unit volume in the mixing region. The amount of beads $Q=nwh\langle v\rangle$ flowing through the mixing region depends only on the rotation speed of the drum if the beads in the solid region do not slip relative to the drum. Therefore, $h=Q/(nw\langle v\rangle)\propto\langle v\rangle^{-1}$. Since a bead will experience larger drag in a more viscous fluid, $\langle v\rangle$ should decrease with μ and hence h should increase with μ. Figures 3(b) and 3(c) show that our experimental measurements of $\langle v\rangle$ and h behave as expected and in qualitative agreement with the previous study by Jain *et al.* [7]. Moreover, the linear relationship between $\langle v\rangle$ and h is verified in the inset of Fig. 3(c). Interestingly, while $\langle v\rangle$ decreases with μ, the data suggest a possible transition point ($\mu\approx10$ mPa s) at which the slope of $\langle v\rangle$ versus μ changes. Such feature is also found in the variation of h in Fig. 3(c). We shall return to this point later.

Although the macroscopic dynamics (characterized by v_s and $\langle v\rangle$) are slower in a more viscous fluid, the microscopic dynamics (represented by the mixing rate of the beads in the drum) behaves differently. The mixing rate is determined by the following procedures. Using imaging software, we partition the high resolution images into cells of

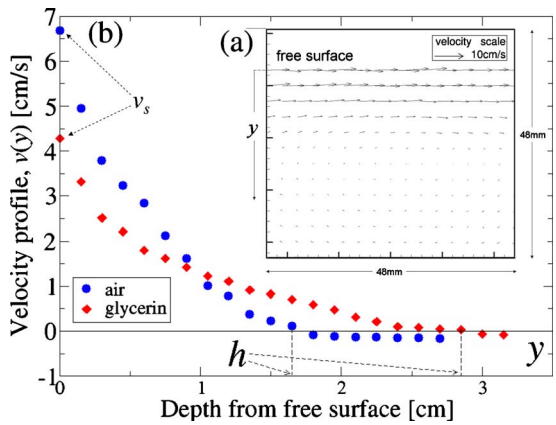

FIG. 2. (Color online) (a) A typical flow field obtained for the dry system in the region of 4.8×4.8 cm^2 near the center of the drum as shown in Fig. 1(a). (b) Velocity profile measured in the dry and the wet ($f=0.8$) system.

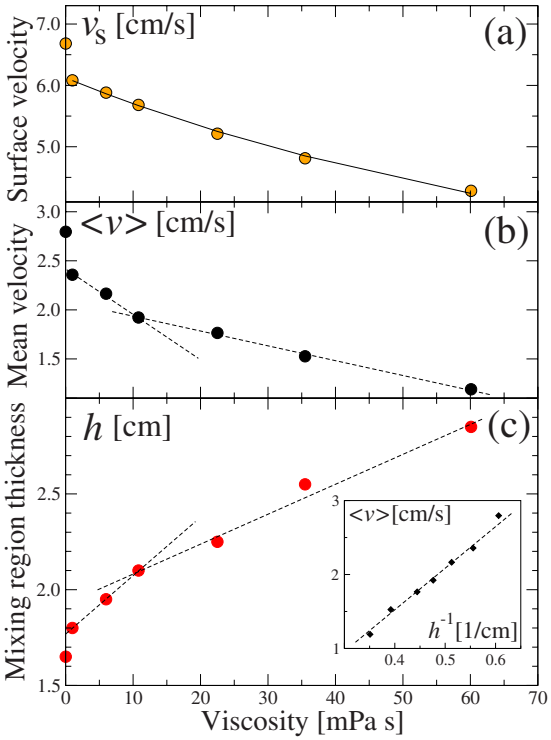

FIG. 3. (Color online) Variations of the (a) surface flow velocity v_s, (b) mean flow velocity $\langle v\rangle$ and (c) the mixing region thickness h with viscosity of the fluid. The curve in (a) is a fit of v_s to the empirical form: $v_s=\frac{a}{1+\mu/b}$. The dotted lines in (b) and (c) are guides to the eyes only. The inset of (c) shows that $\langle v\rangle$ increases linear with h^{-1}.

20 pixel$\times$20 pixel (approximately 1×1 cm^2 in actual dimension). For the cells within the glass beads region, we find the number of pixel n_i occupied by the white beads in the ith cell using a suitable threshold and calculate the white bead fraction $C_i=n_i/400$. The threshold value is chosen such that C_i equals 0 in a cell with no white bead and C_i equals 1 in a cell with no black bead. Then the degree of mixing for the beads in the drum may be indicated by the mixing index M defined as standard deviation of C_i [8,9]. That is, $M=\sqrt{\Sigma_{i=1}^{N}\frac{(C_i-\langle C_i\rangle)^2}{N-1}}$ where N is the number of cell within the glass bead region and $\langle C_i\rangle$ is the average of C_i. For a fully segregated configuration in which half of the cells are totally occupied by the white beads and half of them are totally occupied by the black beads, $M=\frac{N}{2(N-1)}\approx0.5$. In the fully mixed configuration, every C_i equals $\langle C_i\rangle$ and hence, $M=0$.

Figure 4(a) shows the time variations of M for the system of $f=0.5$. One can see that M decreases from an initial value ≈0.45 to a steady value $M_s\approx0.15$ and its temporal variation can be fitted to an exponential decay function [10]: $M(t)=M_oe^{-kt}+M_s$. Note that the initial configuration is carefully prepared so that the black and white beads are completely segregated. Nevertheless, there are cells at the boundary of the drum as well as the boundary between the black bead region and the white bead region whose C_i is neither 0 nor 1. Hence the initial value $M(0)=M_o+M_s<0.5$ is reasonable. On the other hand, M_s does not vanish even at the fully mixed state because of intrinsic statistical fluctuations in C_i.

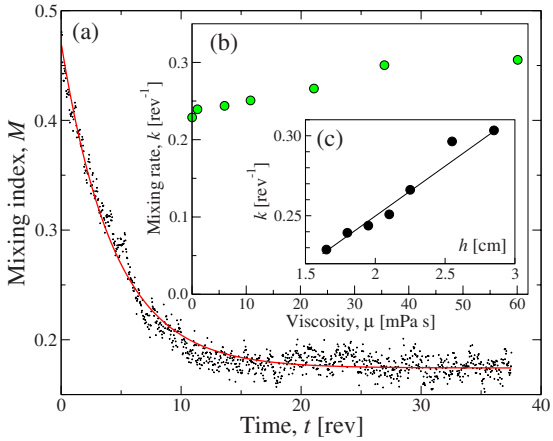

FIG. 4. (Color online) (a) Change of mixing index M with time t for the system of $f=0.5$. Inset (b) shows the change of mixing rate k with respect to the viscosity μ. Inset (c) shows the relation between k and the mixing region thickness h.

Nevertheless, $\langle C_i\rangle$ remains constant and equals 0.47 ± 0.015. The quantity k in the above equation can be considered as the characteristic mixing rate whose value is found to increase with increasing fluid viscosity as shown in Fig. 4(b). In other words, the beads mix faster in a more viscous fluid.

To explain the counter intuitive dependence of the mixing rate on the fluid viscosity, we need to understand the mechanism of mixing in our experiments. When a bead enters the mixing region, it deviates from the average trajectory because of the random motion produced by collisions with other beads [11]. The mean-square displacement of a bead from its average trajectory should be $\langle(\delta y)^2\rangle\approx D\tau$ where D is the diffusion constant and τ is the time that a bead spends in the mixing region. In other words, a bead diffuses a mean distance $\approx\sqrt{D\tau}$ every time it enters and leaves the mixing region. Clearly the time interval between two consecutive beads entering the mixing region is inversely proportional to the rotation speed Γ. Therefore, the time for a bead to diffuse a total distance R is given by $(R/\sqrt{D\tau})(1/\Gamma)$. Since the fraction of the beads in the mixing region is approximately h/R, the total time for every bead to diffuse a distance comparable to the radius of the drum should be $t_{mix}\propto(R/h)(R/\sqrt{D\tau})(1/\Gamma)$. Hence the mixing rate k, which can be identified as t_{mix}^{-1}, should be proportional to $(h/R)(\sqrt{D\tau/R})\Gamma$. From the work of Hill *et al.* [11], the diffusion constant is proportional to $\langle v\rangle d$ and $\tau\propto R/\langle v\rangle$. Therefore we have

$$k\propto(h/R^2)\Gamma\sqrt{\langle v\rangle d\frac{R}{\langle v\rangle}}\propto h\Gamma\sqrt{d/R^3}. \quad (1)$$

Since h increases with the viscosity μ, k increases with μ. In addition, the linear relationship between h and k is also observed as shown in Fig. 4(c). Apparently the viscosity has several effects on the dynamics of our system. Although a more viscous fluid slows down the characteristic speed of a bead and reduces the diffusion rate, it forces the bead to stay longer in the mixing region and at the same time enlarges the

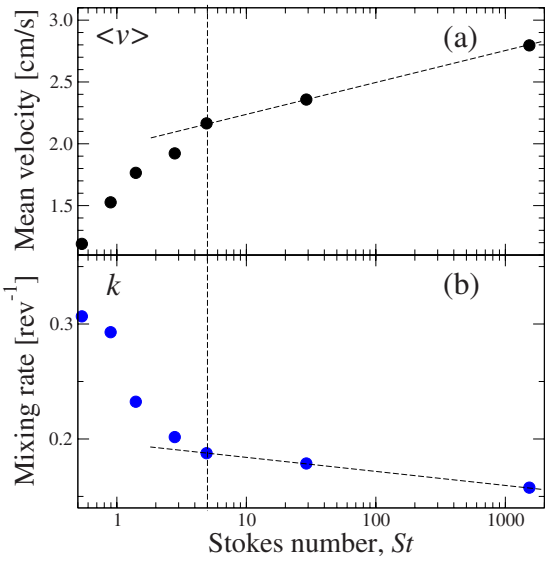

FIG. 5. (Color online) Change of (a) mean velocity $\langle v \rangle$ and (b) mixing rate k with respect to the Stokes number.

mixing region. The overall result is a mixing rate that increases with the viscosity.

Although the diffusive motion of a bead in the mixing region is stochastic, it is governed by the underlying bead motion which may have different dynamical nature when the viscosity of the interstitial fluid is varied. As mentioned before, the variations of $\langle v \rangle$ and h with μ in Figs. 3(b) and 3(c) suggest a transition that may reflect the change in the dynamical nature at $\mu \approx 10$ mPa s. This change may be related to the transition discovered recently by Courrech du Pont *et al.* [6] who found that the particle dynamics in a rotating drum operating in discrete avalanche mode changed from a viscous limit regime to an inertial limit regime when the Stokes number was increased to 5. The Stokes number St $\equiv \sqrt{\rho d^3(\rho - \rho_f)g} \sin \theta / (18\sqrt{2}\mu)$ used in [6], represents the importance of inertial force relative to the viscous force. When we plot the variation of the mean velocity $\langle v \rangle$ and the decay rate k with respective to St (see Fig. 5), sign of a transition is observed at St ≈ 5. However, more works are needed to clarify the transition observed in our experiments. Interestingly, if this finding is indeed the viscous to inertial transition observed by Courrech du Pont *et al.*, then the microscopic flow dynamics will be the same whether the drum is operating in the discrete avalanche flow or in the continuous flow.

To summarize, we have investigated experimentally the granular dynamics immersed in a water-glycerin mixture in a thin rotating drum. We find that the flowing layer becomes thicker, and the mean flow velocity is slower in a more viscous fluid. On the other hand, the particle mixing rate increases with the viscosity of the interstitial fluid. A simple model, in which the mixing region thickness is the dominant parameter to influence the mixing rate in a slurry rotating drum, is introduced to explain the findings. Additionally, a possible transition from the inertial regime to the viscous regime is found on reducing the Stokes number.

The authors would like to thank Professor Chi-Keung Chan and Professor Mario Liu for their valuable comments and suggestions. This research is supported by National Council of Science of Taiwan under Grants No. NSC 95-2112-M-001-030-MY3 and No. NSC 97-2628-E-008-036-MY3.

[1] G. H. Ristow, *Pattern Formation in Granular Materials* (Springer, Berlin, 2000).
[2] J. M. Ottino and R. M. Lueptow, Science **319**, 912 (2008).
[3] J. M. Ottino and D. V. Khakhar, Annu. Rev. Fluid Mech. **32**, 55 (2000).
[4] S. W. Meier, R. M. Lueptow, and J. M. Ottino, Adv. Phys. **56**, 757 (2007).
[5] N. Jain, D. V. Khakhar, R. M. Lueptow, and J. M. Ottino, Phys. Rev. Lett. **86**, 3771 (2001).
[6] S. Courrech du Pont, P. Gondret, B. Perrin, and M. Rabaud, Phys. Rev. Lett. **90**, 044301 (2003).
[7] N. Jain, J. M. Ottino, and R. M. Lueptow, J. Fluid Mech. **508**, 23 (2004).
[8] C. C. Liao, S. S. Hsiau, T. H. Tsai, and C. H. Tai, Chem. Eng. Sci. **65**, 1109 (2010).
[9] D. Shi, A. A. Abatan, W. L. Vargas, and J. J. McCarthy, Phys. Rev. Lett. **99**, 148001 (2007).
[10] J. M. Ottino and D. V. Khakhar, AIChE J. **48**, 2157 (2002).
[11] K. M. Hill, G. Gioia, and V. V. Tota, Phys. Rev. Lett. **91**, 064302 (2003).